European Conference on Optical Communication (ECOC) 2022 © Optica Publishing Group 2022

Nonlinearity Tolerance of Tukey Signalling with Direct Detection

Amir Tasbihi[(1)] and Frank R. Kschischang[(1)]

[(1)] ECE Department, U. of Toronto, Toronto, ON M5S 3G4, Canada {tasbihi,frank}@ece.utoronto.ca

Abstract *We consider Tukey signalling with 50% duty-cycle between ISI-free and ISI-present intervals, and introduce trellis-based codebook design and decoding. The use of an integrate-and-dump detector equips the scheme with a high degree of robustness to nonlinear modulation distortion, making precise waveform shaping unnecessary.*

Introduction

Tukey signalling with direct detection (TSDD) is a data transmission scheme using time-limited waveforms (having a raised-cosine shape in the time domain) to allow amplitude and (to some extent) phase recovery of complex-valued symbols by the deliberate introduction of inter-symbol interference (ISI)[1]. In contrast to intensity-modulation with direct detection (IMDD), TSDD allows information to be encoded in the phase, not only the intensity, of the transmitted symbols; however, this increased capability necessitates implementation of an in-phase/quadrature (IQ) modulator at the transmitter and the use of two (rather than one) analog-to-digital converters (each operating at the baud rate) at the receiver. The requirement of having at least two real-valued samples per complex-valued symbol is inevitable in all schemes that extract phase (in addition to magnitude).

In this paper, we address a number of practical concerns that arise with TSDD. In particular, (1) we consider the influence of the nonlinearity of the IQ modulator (which was previously idealized[1]) and show that the scheme is quite robust to modulator imperfections; (2) we fix the duty-cycle between ISI-free and ISI-present signalling segments to 50% (unlike in previous work[1], where it was allowed to range to values as low as 10%, which leads to unrealistically short integration intervals in high baud-rate systems); (3) we introduce a low-complexity near maximum-likelihood (ML) trellis-based decoding algorithm in the presence of both shot noise and thermal noise encountered at the output of a p-i-n photodiode (PD) under practical parameter settings (replacing the brute-force search decoding and avalanche PD analysis of previous work[1]).

The System Model

The system model is shown in Fig. 1. For simplicity we assume transmission over a single polarization; however, the scheme can be adapted to work in a dual-polarized system. We assume data transmission over a standard single-mode fiber at a wavelength close to 1550 nm. Power loss and chromatic dispersion (CD) are the only fiber imperfections that we take into account.

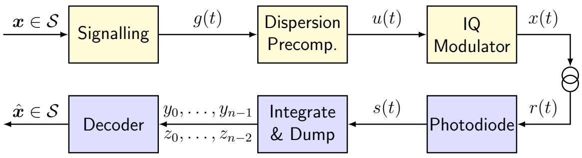

Fig. 1: The system model.

The signalling waveform is a scaled dilated Tukey waveform[1], defined as

$$w(t) \triangleq \begin{cases} \sqrt{\frac{8}{7T}}, & \text{if } |t| \leq \frac{T}{4}; \\ \sqrt{\frac{2}{7T}}\left(1-\sin\left(\frac{\pi(2|t|-T)}{T}\right)\right), & \text{if } \left||t|-\frac{T}{2}\right| \leq \frac{T}{4}; \\ 0, & \text{otherwise,} \end{cases}$$

where T is the reciprocal of the baud rate. The signalling block accepts a complex n-vector $(x_0, \ldots, x_{n-1})$ from the codebook $\mathcal{S} \in \mathbb{C}^n$ as input and produces the waveform $g(t) = \sum_{i=0}^{n-1} x_i w(t - iT)$. Note that $g(t)$ depends only on x_k, $0 \leq k < n$, whenever $|t - kT| \leq T/4$ and depends only on x_ℓ and $x_{\ell+1}$, $0 \leq \ell \leq n-2$, whenever $|t - \ell T - T/2| \leq T/4$. Thus, the time-axis is partitioned into alternating ISI-free intervals $\mathcal{Y}_k$ and ISI-present intervals $\mathcal{Z}_\ell$ as shown in Fig. 2. The integrate-and-dump unit accepts $s(t)$, the noisy output waveform of the photodiode (PD), as its input and produces $y_k = \int_{\mathcal{Y}_k} s(t)\mathrm{d}t$ and $z_\ell = \int_{\mathcal{Z}_\ell} s(t)\mathrm{d}t$.

Due to the uncompensated nonlinearity of the IQ modulator, the implementation of a true ML receiver seems intractable. Instead, at the receiver, we approximate the modulated waveform $x(t)$ as a linear function of the modulating waveform $u(t)$, which becomes increasingly accurate

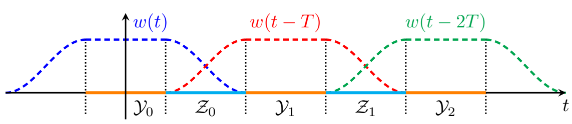

Fig. 2: ISI-free ($\mathcal{Y}_k$) and ISI-present ($\mathcal{Z}_\ell$) intervals.

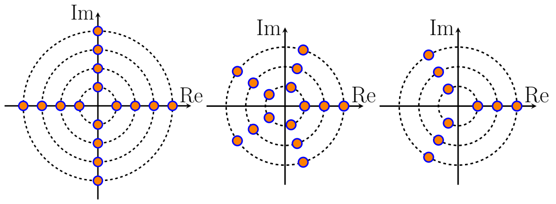

Fig. 3: $(4,4)$-, $(3,5)$-, and $(3,3)$-SQAM constellations.

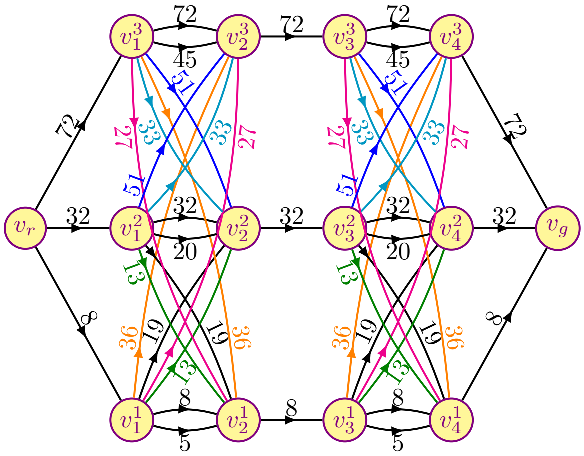

Fig. 4: The trellis for a specific $(3,3)$-SQAM constellation when $n=3$.

for low-power modulating waveforms. Note that this approximation is applied at the receiver, and not at the transmitter, to simplify computations. In all of our numerical simulations, we properly model the nonlinearity of the IQ modulator.

Let $\psi(a,b) \triangleq \frac{1}{4}|a+b|^2 + \frac{1}{8}|a-b|^2$ for all $(a,b) \in \mathbb{C}^2$. The *signature* of any complex n-vector $\boldsymbol{x} = (x_0,\ldots,x_{n-1})$ is defined as $\Upsilon(\boldsymbol{x}) \triangleq (|x_0|^2, \psi(x_0,x_1), |x_1|^2, \psi(x_1,x_2), \ldots, |x_{n-1}|^2) \in \mathbb{R}^{2n-1}$. The noise-free received vector is proportional to $\Upsilon(\boldsymbol{x})$, thus any two transmitted complex-valued n-vectors having the same signature are indistinguishable, even in the absence of noise. It follows that we must choose the elements of the codebook to have different signatures, i.e., to be *square-law distinct* (SLD). SLD sequences drawn from *star-QAM* (SQAM)[2] constellations can be found by a particular trellis diagram.

Trellis Diagrams for SQAM

For a positive integer n_p and a set $\mathcal{R}$ of n_r distinct positive real numbers, the (n_r,n_p)-SQAM constellation with radius set $\mathcal{R}$ and n_p phases is given as $\mathcal{K} = \{re^{i2\ell\pi/n_p} : r \in \mathcal{R}, \ell = 0,1,\ldots,n_p\}$. Fig. 3 shows three examples of SQAM constellations.

For any (n_r,n_p) SQAM constellation $\mathcal{K}$, the set $\Upsilon(\mathcal{K}^n)$ of signatures corresponding to all possible vectors in $\mathcal{K}^n$, can be described using an n_r-state trellis diagram $\mathbb{T}$ of length $2n-1$. The label sequence of a path from the trellis root to the trellis goal is the signature of some $\boldsymbol{x} \in \mathcal{K}^n$ and conversely. For example, Fig. 4 shows the trellis for the $(3,3)$-SQAM constellation with radius set $\mathcal{R} = \{2\sqrt{2}, 4\sqrt{2}, 6\sqrt{2}\}$ when $n=3$.

It can be shown[3] that the number of distinct paths in such a trellis (and therefore the maximum $|\mathcal{S}|$) is $\lceil (n_p+1)/2 \rceil^{n-1} n_r^n$. A coherent detector, on the other hand, can distinguish all $(n_p n_r)^n$ vectors in $\mathcal{K}^n$. For sufficiently large n, the ratio of these quantities drops below two, showing that the rate that can be achieved by an (n_r,n_p)-SQAM constellation under TSDD is at most one bit less than that achieved under coherent detection.

The trellis $\mathbb{T}$ can be used for Viterbi decoding. The output of the integrate-and-dump unit, in the absence of noise, is proportional to the edge labels of $\mathbb{T}$, so a branch metric can be defined[3] to measure the cost associated with the received noisy $(2n-1)$-vector and each directed path in $\mathbb{T}$. It is important to note that, because of PD shot noise, this branch metric is *not* squared Euclidean distance.

Numerical Results

The figures of merit considered here are presented as functions of launch power (LP). To this aim, we use practical values for the parameters of each block in Fig. 1. We have assumed a transmission length of 10 km, an unmodulated laser power of 1 dBm, and the use of an InGaAs p-i-n PD as it gave a better performance than avalanche PDs in our simulations.

We assume a uniformly spaced radius set, *i.e.*, $\mathcal{R} = \{1, 1+\delta, 1+2\delta, \ldots, 1+(n_r-1)\delta\}$ for some positive real δ. Clearly, the performance depends on the choice of δ. Fig. 5 shows the BER of $(8,4)$-SQAM constellations for different values of δ. For these constellations $|\mathcal{S}| = 2^{12}$ and $n=3$; thus, their maximum achievable rate is 4 b/sym. One can see that among the tested δ values, $\delta = 0.2$ has the best performance. A comprehensive table showing the optimal value of δ for different constellations is presented in[3]. For all SQAM constellations used in this section, $\delta = 0.2$ results

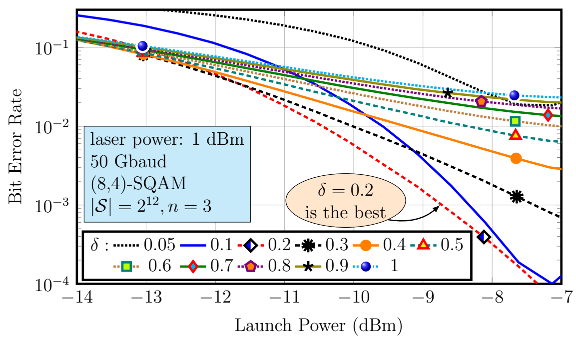

Fig. 5: BER curves for several $(8,4)$-SQAM constellations with $n=3$.

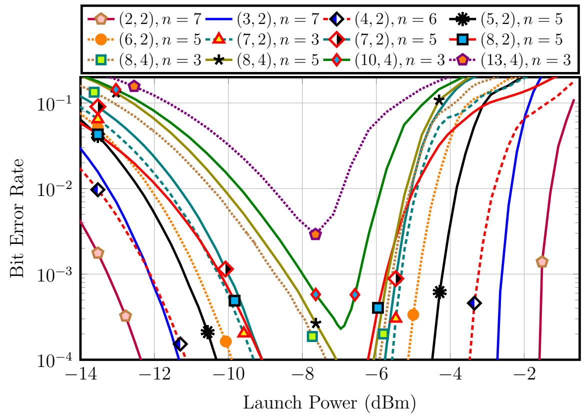

Fig. 6: BER curves for several SQAM constellations at 50 Gbaud rate and with 1 dBm laser power.

in the best performance.

Fig. 6 shows the trellis decoding bit error rate of the proposed scheme for different constellations at 50 Gbaud rate and with 1 dBm laser power. As it is apparent, the BER curves have two parts: 1) a roll-down part where the BER decreases with a higher LP, and 2) a roll-up part which behaves in the opposite manner. The reason for the roll-up part is that the proposed decoder approximates the IQ modulator as being linear, while in fact it is nonlinear. The linear approximation is good when the power of the modulating waveform, $u(t)$, is relatively small. For a fixed laser power, the LP is controlled by $u(t)$; *i.e.,* a high LP demands a higher modulating-waveform power which degrades the accuracy of the approximation. Fortunately, a practical raw BER, *e.g.,* about 10^{-3}, can be achieved in the roll-down area for all considered constellations, except $(13,4)$-SQAM constellation.

We have assumed throughout that $|\mathcal{S}|$ is a power of two, chosen as a subset from all possible SLD sequences. For example, for the $(8,4)$-SQAM constellation with $n=5$, there are 2654208 paths in $\mathbb{T}$, from which we have chosen $2^{21} = 2097152$ SLD sequences to form $\mathcal{S}$.

Fig. 7 shows the theoretically maximum achievable data rate for various SQAM constellations with 50 Gbaud rate, a 1 dBm laser power, and with the power-of-two constraint on $|\mathcal{S}|$. Fig. 7 shows that a desired rate can be achieved using a higher-order constellation along with an error correcting code at a lower LP. For example, while the uncoded $(8,4)$-SQAM constellation with $n=3$ can achieve 4 b/sym at a LP of -9.5 dBm, the same rate can be achieved with a $(10,4)$-SQAM constellation with $n=3$ and an error correcting code of rate $\frac{12}{13}$ at a LP of -12 dBm; resulting in a coding gain of about 2.5 dB.

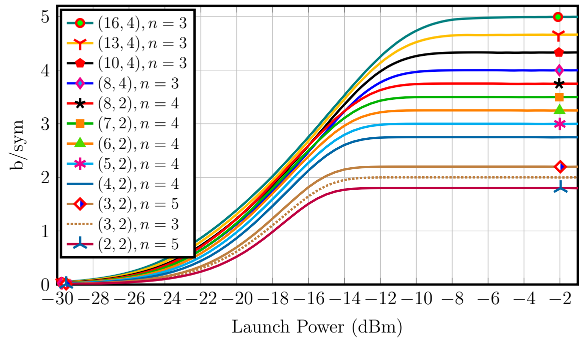

Fig. 7: Achievable data rate for different SQAM constellations at 50 Gbaud and with 1 dBm laser power.

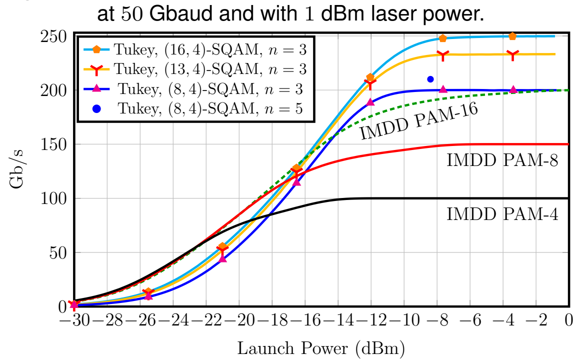

Fig. 8: Throughput for IMDD and the proposed scheme at 50 Gbaud for a single wavelength and a single polarization.

Fig. 8 shows the throughput of the proposed and the IMDD schemes at 50 Gbaud. While the $(8,4)$-SQAM TSDD achieves a throughput of 200 Gb/s at a LP of -10 dBm, IMDD with PAM-16 achieves this rate at about 0 dBm; thus, by using the proposed scheme a gain of about 8 dB can be achieved compared to the IMDD scheme. We can achieve the same throughput by using a $(16,4)$-SQAM with $n = 3$ and an error correcting code of rate 0.8 at a LP of -12.9 dBm, as well, *i.e.*, a 2.9 dB coding gain. Furthermore, Fig. 8 shows that for a fixed LP and a fixed baud rate one may achieve higher throughputs by using the proposed scheme rather than IMDD. For example, at 50 Gbaud and a LP of -10 dBm, the proposed scheme achieves a throughput of 200 Gb/s with an $(8,4)$-SQAM and $n = 3$, while an IMDD scheme achieves only about 145 Gb/s with a PAM-8 constellation.

Conclusions

Comparisons with IMDD show that at 50 Gbaud and at a LP of -10 dBm, TSDD achieves a throughput of 225 Gb/s and 200 Gb/s using $(13,4)$-SQAM and $(8,4)$-SQAM constellations, respectively, while IMDD achieves 145 Gb/s using PAM-8. This increase in throughput requires implementing an IQ modulator at the transmitter and two ADCs, each operating at the baud rate, at the receiver.

References

[1] A. Tasbihi and F. R. Kschischang, “Direct detection under Tukey signalling”, *J. Lightwave Techn.*, vol. 39, no. 21, pp. 6845–6857, Nov. 2021.

[2] D. Plabst, T. Prinz, T. Wiegart, T. Rahman, N. Stojanović, S. Calabrò, N. Hanik, and G. Kramer, “Achievable rates for short-reach fiber-optic channels with direct detection”, *J. Lightwave Techn.*, Feb. 2022, (Early Access version).

[3] A. Tasbihi and F. R. Kschischang, “Practical considerations in direct detection under Tukey signalling”, arXiv:2204.13806, Mar. 2022.